IOP Conference Series: Earth and Environmental Science

PAPER • **OPEN ACCESS**

Modeling and Controller Design of Flyback Converter Operating in DCM for LED Constant Current Drive

Modeling and Controller Design of Flyback Converter Operating in DCM for LED Constant Current Drive

Wei Feng[1], Yiwen Chen[1*], Jiahui Jiang[2]and Weiting Jiang[1]

[1]College of Electrical Engineering and Automation Department, Fuzhou University, Fuzhou, Fujian Province,350108,China

[2]College of Electrical Engineering, Qingdao University, Qingdao, Shandong Province, 266071, China

[*]Corresponding author's e-mail:fzucyw@163.com

Abstract. In power converter, the system model has a significant meaning of the design of the controller and the dynamic characteristics. In this paper, the switching network average method is used to set up the small signal model of flyback circuit, which is operating in discontinuous current mode(DCM). A controller with single zero and single pole is designed based on the small signal model which is set up in this paper. Moreover, the analysis of system stability and dynamic response is proposed. Finally, the system is simulated and verified by a flyback LED constant current drive circuit (220AC input, 0.7A/16W output).

1. Introduction

Modeling and Simulation of power electronics is an important method of power converter controller design,and also one of the research directions of power electronics technology [1-3]. The high-power DC/DC converter usually operates in continuous current mode(CCM). In reference [4],the energy conservation method is used to model and analyze the small signal of flyback circuit in CCM. In reference [5-6],the state space average method and Euler formula are used to establish the small signal model of the forward converter in CCM. In reference [7], the flyback converter operatedat 1 MHz switching frequencyestablishes the small signal model by the state space average method. In reference [8], theaveraged nonlinear model is established for flyback converter which adapts nonlinear model predictive controlmethod. In reference [9],small-signal model of flyback converter in continuous-conduction mode(CCM) with peak-current control at variable switching frequency is proposed.However, the low-power DC/DC converter usually works in the state of discontinuous current mode (DCM). In order to better design the controller of the system and obtain better output accuracy and dynamic performance, it is necessary to set up small signal modeling for converter working in DCM.

In this paper, the small signal model of flyback circuit in DCM is established by the switching network average method. According to the small signal model, the controller is designed and finally verified by simulation and experiment.

2. Working mode analysis and small signal modelling

The topology equivalent circuit of the flyback converter is shown in Figure 1.The transformer adopts the parallel equivalent of magnetizing inductance and ideal transformer.Switching devices in the diagram are considered as ideal. According to the working principle of flyback circuit in DCM, the working mode which is divided into three stages and the working waveform are shown in Figure 2 and Figure 3 respectively.Among the above two pictures, equivalent inductance current i_L ,voltage at both ends v_L, and i_1 、 v_1 、 i_2 and v_2 in the switch network are showed.

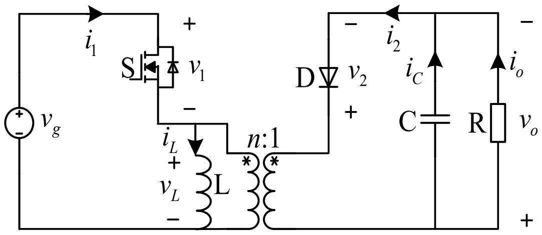

Figure 1. Topology of flyback converter

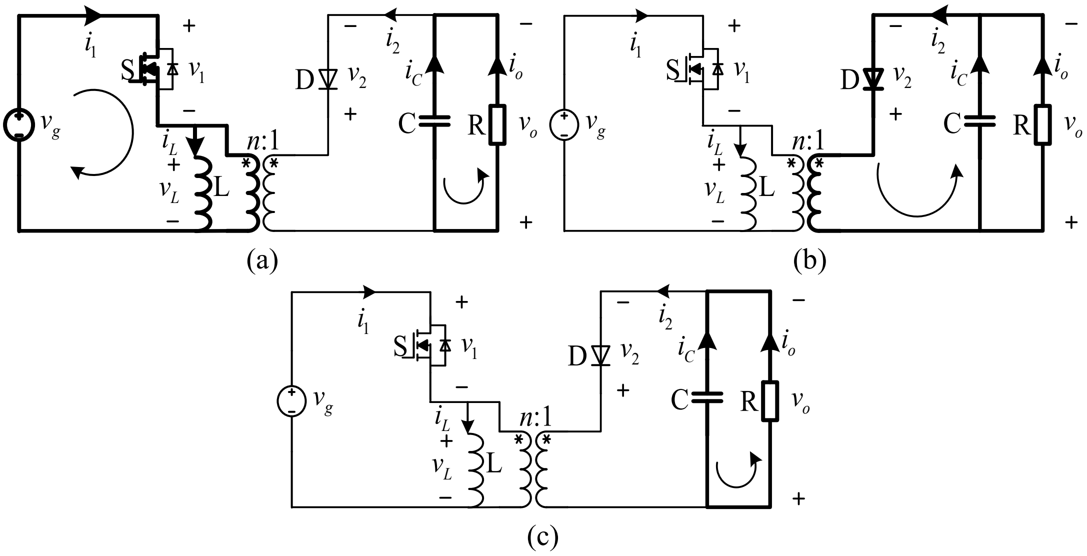

Figure 2. Equivalent circuit of flyback in DCM

From Figure 3, the following equation can be obtained.

$$d_1 + d_2 + d_3 = 1 \tag{1}$$

$$i_{1pk} = \frac{< v_g(t) >_{T_s}}{L} d_1 T_s \tag{2}$$

The state space average model of switching network is shown in equation (3).

$$\begin{cases} < v_1(t) >_{T_s} =< v_g(t) >_{T_s} \\ < i_1(t) >_{T_s} = \dfrac{d_1^{\,2}(t) T_S < v_1(t) >_{T_s}}{2L} \\ < v_2(t) >_{T_s} =< v_o(t) >_{T_s} \\ < i_2(t) >_{T_s} = \dfrac{d_1^{\,2}(t) T_s}{2L} \dfrac{< v_1(t) >^2_{T_s}}{< v_2(t) >_{T_s}} \end{cases} \tag{3}$$

Apply a small disturbance to each parameter as show inequation (4).

$$\begin{cases} v_1(t) = V_1 + \hat{v}_1 \\ v_2(t) = V_2 + \hat{v}_2 \\ i_1(t) = I_1 + \hat{i}_1 \\ i_2(t) = I_2 + \hat{i}_2 \\ d_1(t) = D + \hat{d} \\ v_g(t) = V_g + \hat{v}_g \\ v_o(t) = V_o + \hat{v}_o \end{cases} \tag{4}$$

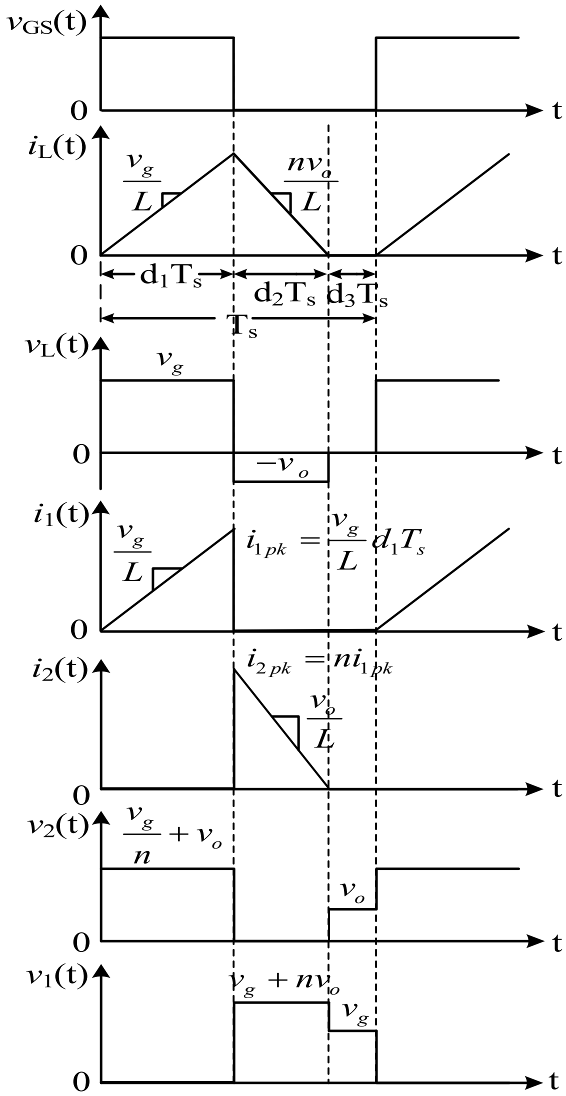

Figure 3. Operating waveforms

Assuming that the dynamic disturbance component is far less than the steady-state component, the first-order disturbance effect is retained and the higher-order parameter disturbance is ignored. the steady-state equations of the converter are further obtained, as shown in equation (5).

$$\begin{cases} D = \dfrac{I_o}{V_g}\sqrt{\dfrac{2RL}{T_s}} \\ V_1 = V_g \\ V_2 = V_o = I_o R \\ I_1 = \dfrac{T_s D^2 V_1}{2L} \\ I_2 = \dfrac{T_s D^2 V_1^{\,2}}{2LV_2} \end{cases} \tag{5}$$

According to (3)-(5),the small signal equations are obtained as shown in equation (6).

$$\begin{cases} \hat{v}_1 = \hat{v}_g \\ \hat{v}_2 = \hat{v}_o = \hat{i}_o R \\ \hat{i}_1 = \dfrac{DV_1T_s}{L}\hat{d} + \dfrac{D^2T_s}{2L}\hat{v}_1 \\ \hat{i}_2 = \dfrac{DT_sV_1^2}{LV_2}\hat{d} + \dfrac{D^2T_sV_1}{LV_2}\hat{v}_1 + \dfrac{D^2T_s}{2L}\left(\dfrac{V_1}{V_2}\right)^2\hat{v}_2 \end{cases} \tag{6}$$

3. Analysis of small signal AC model

From equation (6), the small signal AC equivalent model of the converter can be obtained as shown in Figure 4,in which $r_1 = \dfrac{2L}{D^2T_s}$, $j_1 = \dfrac{DT_sV_1}{L}$, $r_2 = \dfrac{2L}{D^2T_s}\left(\dfrac{V_2}{V_1}\right)^2$, $j_2 = \dfrac{DT_sV_1^2}{LV_2}$, $g_2 = \dfrac{D^2T_sV_1}{LV_2}$.

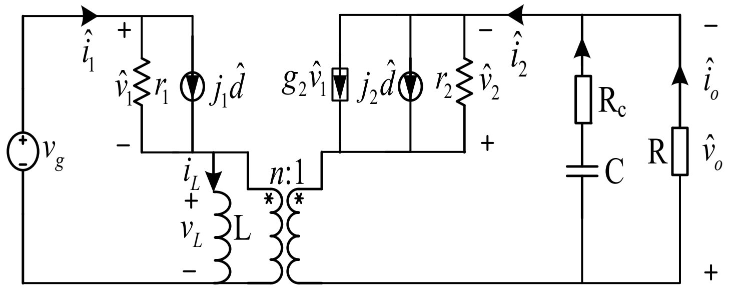

Figure 4.Ideal small signal model of flyback converter

According to KCl / KVL law, control (d) - output (i_o) transfer function can be obtained and the simplified equation is shown in (7).

$$G_{id} = G_{id0}\frac{\left(1+\dfrac{s}{\omega_0}\right)\left(1+\dfrac{s}{\omega_1}\right)}{\left(1+\dfrac{s}{\omega_2}\right)\left(1+\dfrac{s}{\omega_3}\right)} \tag{7}$$

In equation (7), $G_{id0} = V_1\sqrt{\dfrac{T_s}{2RL}}$, $\omega_0 = \dfrac{1}{R_cC}$, $\omega_1 = -\dfrac{nV_1^2}{nLRI_o^{\,2} + LI_oV_1}$, $\omega_2 = \dfrac{2}{RC + 2R_cC}$, $\omega_3 = \dfrac{V_1^2}{RLI_o^{\,2}}$.

From the transfer function, it can be seen that the system has a zero point in the left half plane, a zero point in the right half plane and two poles in the left half plane.

4. Example analysis

4.1Closed-loop design

The design of prototype uses the ICE3B0565J IC of Infineon and the single zero point single pole controller. The controller circuit and the closed-loop transfer function of the system are shown in Figure 5 and Figure 6, respectively.

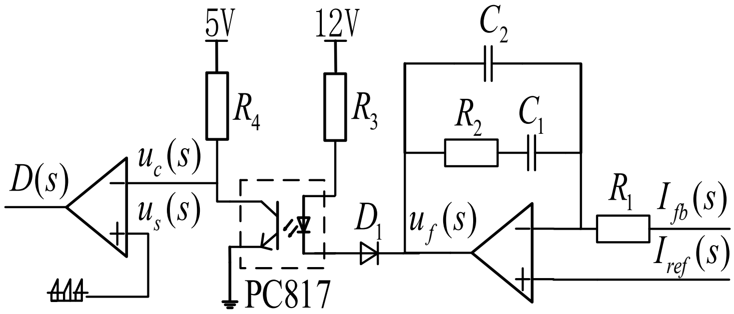

Figure 5.Circuit of controller

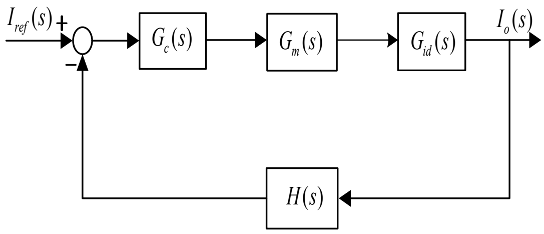

Figure 6.The system closed-loop transfer function

$G_{id}(s)$ is the duty cycle of the converter to the output transfer function. $G_c(s)$ is transfer function of controller. $G_m(s)$ is transfer function for PWM pulse width modulator. $H(s)$ is the transfer function of feedback. In addition, the transfer function of the controller is shown in equation (8).

$$G_c(s) = \frac{k_p(T_z s + 1)}{s(T_p s + 1)} \tag{8}$$

Where $k_p = \frac{1}{R_1(C_1 + C_2)}$, $T_z = R_2 C_2$, $T_p = \frac{C_1 C_2 R_2}{C_1 + C_2}$.

According to Figure 5:

$$u_c(s) = 5 - \frac{12 - V_F - V_D - u_f(s)}{R_3} R_4 C_{CTR} \tag{9}$$

According to the literature [10]:

$$u_s(s) = 3.2\frac{V_g}{L} R_s T_s d(s) + 0.6 \tag{10}$$

Where R_s is sampling resistance for series in the original winding.Let

$$u_c(s) = u_s(s) \tag{11}$$

Add disturbance to the duty cycle d and u_f :

$$\begin{cases} u_f = U_f + \hat{u}_f \\ d = D + \hat{d} \end{cases} \tag{12}$$

The steady-state equation can be obtained and is shown in equation (13).

$$D = \frac{4.4-(12-V_F-V_D-U_f)\frac{R_4C_{CTR}}{R_3}}{3.2\frac{V_g}{L}R_sT_s} \tag{13}$$

The small signal equation is shown in equation (14).

$$\hat{d} = \frac{R_4C_{CTR}L}{3.2V_gR_sR_3T_s}\hat{u}_f \tag{14}$$

According to equation (14):

$$G_m(s) = \frac{R_4C_{CTR}L}{3.2V_gR_sR_3T_s} \tag{15}$$

Where $H(s)$ is the scaling of the current sampling, i.e. the output current sampling resistance, so,

$$H(s) = R_{sam} \tag{16}$$

Original loop gain function:

$$G_0(s) = G_m(s)G_{id}(s)H(s) \tag{17}$$

Loop gain function after compensation:

$$G(s) = G_c(s)G_0(s) \tag{18}$$

4.2Experimental verification

Parameters of the main circuit is shown in Table 1. According to Table 1,the original loop gain function can be simplified as shown in equation (19).

$$G(s) = \frac{-6.1689e^{-3}(s-5.567e^5)(s+5e^4)}{(s+1.391e^6)(s+61.18)} \tag{19}$$

Table 1. Parameters of the main circuit

Description	**Symbol**	**Value**
Input voltage	V_g	220V
Output current	I_O	0.7A
Input capacitance	C_{in}	47uF
Switching period	T_s	1/67ms
Primary inductor	L	4.43mH
Turn ratio of transformer	n:1	110/12
Primary sampling resistance	R_s	0.975Ω
Output sampling resistance	R_{sam}	0.3Ω
Output filter capacitance	C_{out}	1000uF
Output filter capacitance ESR	R_C	0.02Ω
Output power	P_{out}	16W

The corresponding Bode diagram is shown in Figure 7.

According to Figure 7,it is can be seen that the gain crossover frequency and phase margin are 17.1hz and 120 ° respectively. Although the system is stable, the system bandwidth and the gain crossover frequency is too small, resulting in the dynamic performance is poor.

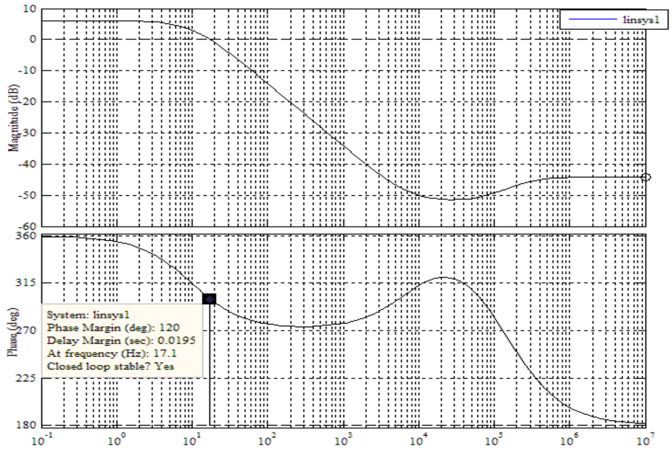

Figure 7. The Bode diagram of original loop gain function

Therefore, the single pole single zero controller is designed to adjust the output accuracy, voltage regulation rate, band width and dynamic performance of the system. The main parameters of the single zero point single pole controller are shown in Table 2.

Table 2.Parameters of the controller

Parameter	**Value**
R_1	1 KΩ
R_2	75 KΩ
C_1	220 nF
C_2	47 pF
R_3	2 KΩ
R_4	15 KΩ

After adding the controller, the loop gain function of the system is shown in equation (20).The Bode diagram of the loop gain function is shown in Figure8.

$$G(s)=\frac{-1.3125e^{5}(s-5.567e^{5})(s+5e^{4})(s+45.45)}{s(s+61.18)(s+2.128e^{5})(s+1.391e^{6})} \tag{20}$$

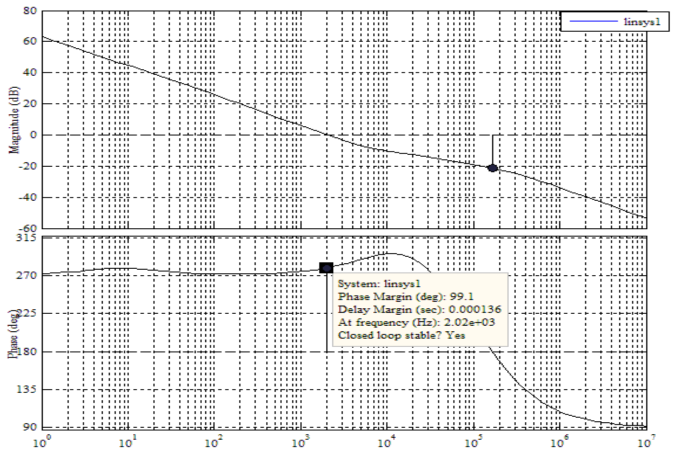

Figure 8. The Bode diagram of loop gain functionafter adding the controller

The closed-loop simulation of the system is carried out by using PSIM software, and the output current waveform is shown in Figure9.

The experimental waveform and prototype experiment platform are shown in Figure10 and Figure11, respectively.

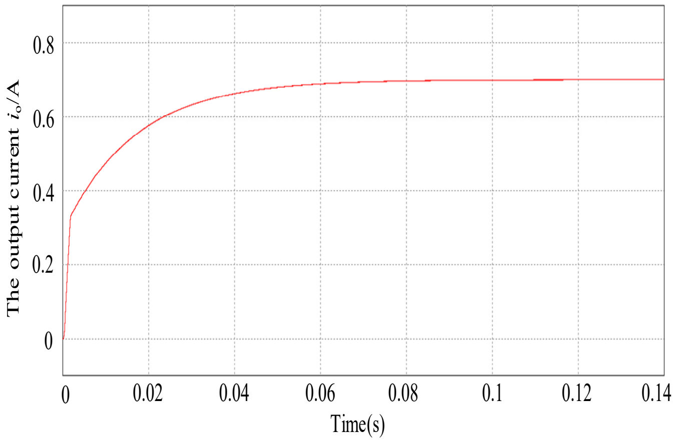

Figure 9. The output current waveform by simulation

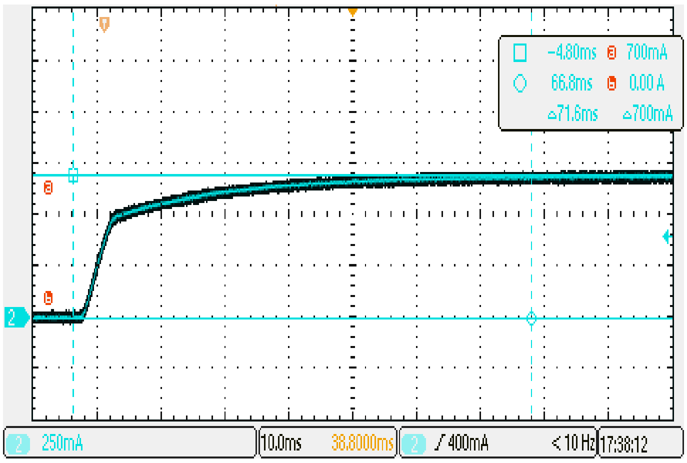

Figure 10. The output current waveform of experiment

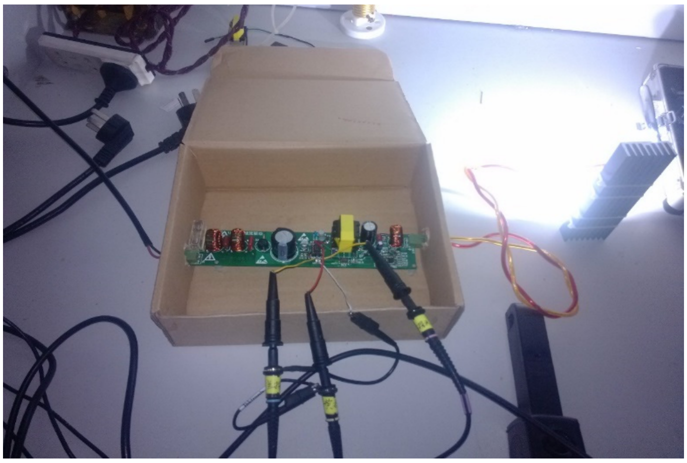

Figure 11.Prototype experiment platfor

5. Conclusion

In this paper, the small signal modeling of flyback converter in DCM is proposed, and the switching network average method is used to solve the small signal model. This modeling method can also be extended to other DC / DC converters. It is found that the modeling of the controller is helpful to the analysis of the characteristics of the converter and the design of the controller. Compared with the traditional PI controller, the single zero and single pole controller has better high frequency characteristics. The experimental results are basically consistent with the simulation results, which verify the feasibility and accuracy of the small signal modeling.

Acknowledgments
The work was supported by Natural Science Foundation Project in Fujian Province of China (2018j01757).

References

[1] Pan, S., Pahlevaninezhad, M., Jain, P. K. (2014, March) Series resonant converters with an adaptive secondary-side digital control for MHz 48V VRs: Circuit analysis and modeling. In:2014 IEEE Applied Power Electronics Conference and Exposition. Texas.pp. 20-26.
[2] Yang, T.,Bozhko,S.,Asher,G. (2015)Active front-end rectifier modelling using dynamic phasors for more-electric aircraft applications .Electrical Systems in Transportation IET.J.IEEE. Commun.,5:77-87
[3] Nahvi, S.A., Bazaz,M.A., Khan,H.(2017) Model order reduction in power electronics: Issues and perspectives. In:2017 International Conference on Computing, Communication and Automation. Greater Noida.pp. 1417-1421
[4] Akbarabadi, S.A., Atighechi,H., Jatskevich.J.(2013)Circuit-averaged and state-space-averaged-value modeling of second-order flyback converter in CCM and DCM including conduction losses.In:Fourth International Conference on Power Engineering.Xiamen.pp. 995-1000.
[5] Yang,R.(2018)A Practical Small Signal Model for the Interleaved Parallel-Series Active Clamp Forward Converter With Peak Current Control.In:2018 IEEE International Power Electronics and Application Conference and Exposition. Shenzhen.pp.1-7.
[6] Andreescu, G.D., Cornea, O., Muntean, N., Guran, E.. (2015). Bidirectional Flyback Inverter with Low Output Voltage THD. In Jubilee IEEE Int Symposium on Applied Computational Intelligence and Informatics. Timisoara. pp.95-99.
[7] Gu, D.L., Xi,J.X., He, L.N.(2019) A Digital PWM Controller of MHz Active Clamp Flyback with GaN Devices for AC-DC Adapter.In: the IEEE Industrial Electronics Society. Lisbon. pp.1496-1501.
[8] Tahami, F., Abedi, M.R., Rezaei,K.(2011) Optimum nonlinear model predictive controller design for Flyback PFC rectifiers. In: 2010 IEEE Symposium on Industrial Electronics and Applications.Penang. pp.70-75.
[9] Cheng, C.H., Chen, C.J., Wang, S.S.(2017) Small-signal model of flyback converter in continuous-conduction mode with peak-current control at variable switching frequency. J. IEEE.Commun., 33(5): 4145-4156.
[10] AG, I.T.(2013) Off-Line SMPS Currrent Mode Controller with integrated 650V CoolMOS and Startup cell (frequency jitter Mode) in DIP-8.